

ViP: Virtual Pooling for Accelerating CNN-based Image Classification and Object Detection

Zhuo Chen¹ Jiyuan Zhang¹ Ruizhou Ding¹ Diana Marculescu¹

Abstract

In recent years, Convolutional Neural Networks (CNNs) have shown superior capability in visual learning tasks. While accuracy-wise CNNs provide unprecedented performance, they are also known to be computationally intensive and energy demanding for modern computer systems. In this paper, we propose Virtual Pooling (ViP), a model-level approach to improve speed and energy consumption of CNN-based image classification and object detection tasks, with a provable error bound. We show the efficacy of ViP through experiments on four CNN models, three representative datasets, both desktop and mobile platforms, and two visual learning tasks, *i.e.*, image classification and object detection. For example, ViP delivers **2.1x** speedup with less than 1.5% accuracy degradation in ImageNet classification on VGG-16, and **1.8x** speedup with 0.025 mAP degradation in PASCAL VOC object detection with Faster-RCNN. ViP also reduces mobile GPU and CPU energy consumption by up to **55%** and **70%**, respectively. Furthermore, ViP provides a knob for machine learning practitioners to generate a set of CNN models with varying trade-offs between system speed/energy consumption and accuracy to better accommodate the requirements of their tasks. Code is publicly available.

1. Introduction

Deep Convolutional Neural Networks (CNNs) have gained tremendous traction in recent years thanks to their outstanding performance in visual learning tasks, *e.g.*, image classification and object detection. However, CNNs are often considered very computationally intensive and energy demanding (Lebedev et al., 2014; Han et al., 2015; Cai et al., 2017). With the prevalence of mobile devices, being able to run CNN-based visual tasks efficiently, in terms of both

¹Department of Electrical and Computer Engineering, Carnegie Mellon University, Pittsburgh, USA. Correspondence to: Zhuo Chen <zhuochen@cmu.edu>.

speed and energy, becomes a critical enabling factor of various important applications, *e.g.*, augmented reality, self-driving cars, Internet-of-Things, *etc.*, which all heavily rely on fast and low energy CNN computation. To alleviate the problem, engineers and scientists proposed various solutions, including sparsity regularization, connection pruning, model quantization, low rank approximation, *etc.* In this work, we propose a complementary approach, called *Virtual Pooling* (ViP), which takes advantage of pixel locality and redundancy to reduce the computation cost originating from the most computationally expensive part of CNN: convolution layers (conv layers). As illustrated in Figure 1, ViP reduces computation cost by computing convolution with a larger (2x) stride size. While naturally this operation quickly shrinks the output feature map, and thus can only be done a few times before the image vanishes, we overcome this problem by recovering the feature map via *linear interpolation* with provable error bound. The succeeding layer hence observes the same size of input with or without ViP, and no architectural change is needed. Our experimental results on different CNN models and tasks show that we can achieve **2.1x** speedup with 1.5% accuracy degradation in image classification, compared to the 1.9x speedup with 2.5% degradation from the prior work (Figueroa et al., 2016), and **1.8x** speedup with 0.025 mAP degradation in object detection.

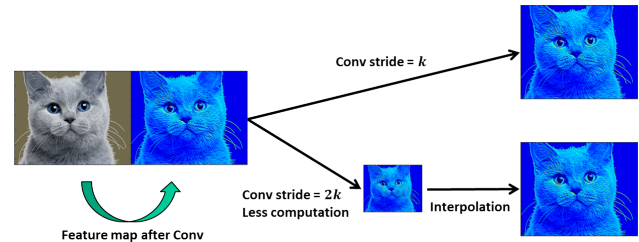


Figure 1. Illustration of virtual pooling (LinkViz). By using a larger stride, we save computation in conv layers and, to recover the output size, we use linear interpolation which is fast to compute.

2. Related Work and Contributions

There are several prior works targeting CNN acceleration (Han et al., 2015; Wen et al., 2016; Figuroa et al., 2016; Ding et al., 2017). Model compression (Han et al., 2015; Wen et al., 2016; He et al., 2018a;b) is a popular approach of

reducing CNN memory requirement and runtime via weight pruning. (Han et al., 2015) proposed to prune connections and fine-tune the network progressively which results in high compression rate. However, due to the non-structured sparsity generated by this method, it also needs specialized hardware to realize high speedup (Han et al., 2016a). In light of this, (Wen et al., 2016) used group lasso to generate structured sparsity and speed up CNNs on general-purpose processors, *e.g.*, CPU and GPU.

CNN model binarization or quantization methods (Courbariaux et al., 2015; 2016; Ding et al., 2017; Wu et al., 2016; Zhou et al., 2017; Zhu et al., 2016) quantize CNN weights and/or activations into low-precision fewer-bit representations. Thereafter, they are able to both reduce memory cost and speedup computation by using efficient hardware units. (Courbariaux et al., 2015) uses binary weights rather than continuous-valued weights in CNN models, which is not only able to save memory space, but also greatly speedup convolution via replacing multiply-accumulate operations by simple accumulations. Ding *et al.*, (Ding et al., 2017) reduces the number of bits of CNN weights through its binary representation, which can be sped up by using shift-add operation rather than expensive multipliers on hardware. (Courbariaux et al., 2016; Rastegari et al., 2016) further quantize the CNN intermediate activations, resulting in both binary weight and input, which can be further accelerated via efficient XNOR operation.

Low rank approximation methods (Jaderberg et al., 2014; Lebedev et al., 2014; Denton et al., 2014) speed up convolution computation by exploiting the redundancies of the convolutional kernel using low-rank tensor decompositions. The original conv layer is then replaced by a sequence of conv layers with low-rank filters, which have a much lower total computational cost. (Jaderberg et al., 2014) exploit cross-channel or filter redundancy to construct rank-one basis of filters in the spatial domain. (Lebedev et al., 2014) use non-linear least squares to compute a low-rank CP-decomposition of the filters into fewer rank-one tensors and then fine-tune the entire network.

The closest work to ours is PerforatedCNNs (Figurnov et al., 2016) which, inspired by the idea of loop perforation (Sidiropoulos-Douskos et al., 2011), reduces the computation cost in conv layers by exploiting the spatial redundancy. Nevertheless, PerforatedCNNs use a dataset dependent method to generate an irregular output mask that determines which neuron should be computed exactly. In addition, PerforatedCNNs need a mask, and hence loading overhead, at runtime to determine the value for interpolation, while ViP only depends on the intermediate activations of the CNN layer without extra parameters. Finally, PerforatedCNNs also considered the use of a pooling-structured mask, but it can only be applied to the layers immediately

preceding a pooling layer and the associated interpolation method is nearest neighbor. In contrast, our method can be applied to any conv layer in the network. Furthermore, we can show that the ViP method achieves higher speedup with lower accuracy degradation. To the best of our knowledge, our work makes the following contributions:

1. We are the first to propose and implement the Virtual Pooling (ViP) method with provable error bound. ViP is independent of the dataset and can be applied to accelerate any conv layer.
2. Plug-and-play: ViP is a self-contained custom layer. Without modifying the deep learning framework, it works simply by doubling the stride of the conv layer and inserting the ViP layer after it.
3. More than providing a single CNN configuration, ViP can generate a set of CNN models with varying speedup/energy-accuracy trade-offs that a machine learning practitioner can select the right model for the task at hand.
4. Most CNN acceleration techniques consider only the image classification task, while they lack evidence on how their performance may translate to the object detection task, which has its own unique properties. In this work, we conduct experiments to show that ViP also works well under the state-of-the-art faster-rcnn object detection framework.

The remainder of this paper is organized as follows. Section 3 introduces the details of the virtual pooling method. In Section 4, we conduct extensive experiments with different CNN models on both desktop and mobile platforms, and we apply ViP to speed up both image classification and object detection tasks. Finally, we conclude our work in Section 5.

3. Methodology

Virtual Pooling (ViP) relies on the idea of reducing CNN computation cost by taking advantage of pixel spatial locality and redundancy. CNNs are often comprised of multiple conv layers interleaved with pooling layers. Pooling layers are considered essential for reducing spatial resolution such that computation cost is reduced and robustness to small distortions in images is enhanced. However, the widely-used stride-two non-overlapping pooling method (Simonyan & Zisserman, 2014; He et al., 2016) reduces image size by half in each of the two dimensions, and thus quickly shrinks the image. As a result, the maximum number of pooling operations that can be done in a CNN is limited by the size of the input image. For example, an input image of size $224 * 224$ is shrunk to size $7 * 7$ after only five pooling layers in VGG-16, while the current state-of-the-art CNNs usually have several tens to hundreds of layers (Simonyan & Zisserman, 2014; He et al., 2016). There is an opportunity to reduce computation further if we can bridge the gap

between the number of pooling-like operations we can do and the number of layers in the network.

3.1. ViP Layer

To this end, we propose ViP, a method that can maintain the output size of each layer, while using a larger-stride convolution. Consequently, we can have as many ViP layers as possible while not encountering the problem of diminishing image size in the real pooling operation. While it is possible to increase the stride of an early layer and remove a later pooling layer to achieve a similar effect, our experiments show that ViP is constantly better than pooling removal with 1.42% higher accuracy on average. Furthermore, this method can only reduce computation in consecutive conv layers prior to pooling, while ViP works in any order (as we will show later, accuracy sensitivity is non-monotonic with the network layer) which gives a better accuracy-speedup curve. As illustrated in Figure 1, ViP saves computation by performing a larger stride convolution in the layer before ViP, and then recovers the output size by simple linear interpolation which is very computationally efficient. For example, by applying ViP after each conv layer of VGG-16, we can double the stride of preceding conv layer to reduce computation, and recover the image size by linear interpolation. Therefore, the succeeding layer observes the input of exactly the same size. Furthermore, the theoretical speedup of this approach is 4x because we reduce the number of convolutions by half in each of the two dimensions of the input. Although transposed convolution (Deconv) (Long et al., 2015) is also an upsampling method with similar functionality as linear interpolation, to speedup the network, its overhead must be sufficiently small so it does not offset the reduced latency due to the larger-stride convolution. In the supplementary material we show that ViP is very efficient and its computation is only 0.016% of Deconv.

To be more specific, let's use \mathcal{I} to denote the input to conv layer and \mathcal{O} to denote the output. Without loss of generality, although \mathcal{I} and \mathcal{O} are often four-dimensional, we omit the first dimension of batch index because ViP applies to all images in the batch independently, and therefore, $\mathcal{I}_{c,h,w}$ and $\mathcal{O}_{c,h,w}$ both have three dimensions: channel $c \in [1, C]$, height $h \in [1, H]$, and width $w \in [1, W]$. We consider convolution filters, $\mathcal{W}_{c',c,m,n}$, with the same height and width with odd values M as are commonly used in CNNs (Simonyan & Zisserman, 2014; He et al., 2016), and with c' representing the index of the filter. For the purpose of simplicity, we further assume H and W are even numbers, e.g., input image size of ImageNet is usually $224 * 224$, and in the case of odd numbers, we have special cases only on the boundaries of the image that are easy to deal with. Furthermore, we use $\mathcal{O}_{c',h,w}^{Orig}$ to represent the output of the original stride- s convolution without ViP, and $\mathcal{O}_{c',h,w}^{ViP}$ to denote the output of using ViP method, i.e., the output of

stride- $2s$ convolution plus linear interpolation. A smaller $\|\mathcal{O}_{c',h,w}^{Orig} - \mathcal{O}_{c',h,w}^{ViP}\|_2$ indicates a smaller perturbation of the truth output and hence, less accuracy degradation for the ViP method. According to the definition of convolution:

$$\mathcal{O}_{c',h,w}^{Orig} = \sum_{c=1}^C \sum_{m,n=-\lfloor \frac{M}{2} \rfloor}^{\lfloor \frac{M}{2} \rfloor} \mathcal{I}_{c,s \cdot h-m, s \cdot w-n} * \mathcal{W}_{c',c,m,n} \quad (1)$$

If we double the stride, we have an output with reduced size:

$$\mathcal{O}_{c',h,w}^{Red} = \sum_{c=1}^C \sum_{m,n=-\lfloor \frac{M}{2} \rfloor}^{\lfloor \frac{M}{2} \rfloor} \mathcal{I}_{c,2s \cdot h-m, 2s \cdot w-n} * \mathcal{W}_{c',c,m,n} \quad (2)$$

For ease of explanation, we use an auxiliary function $\mathcal{O}_{c',h,w}^{Zero}$ which is zero-spaced to enlarge $\mathcal{O}_{c',h,w}^{Red}$ to the same size of $\mathcal{O}_{c',h,w}^{Orig}$ in the following way:

$$\mathcal{O}_{c',h,w}^{Zero} = \begin{cases} \mathcal{O}_{c',h/2,w/2}^{Red} & h, w \text{ are even numbers} \\ 0 & \text{Otherwise} \end{cases} \quad (3)$$

We approximate the output with the ViP method $\mathcal{O}_{c',h,w}^{ViP}$ by using the mean of its immediate non-expanding-zero neighbors (including itself, if computed exactly) in $\mathcal{O}_{c',h,w}^{Zero}$:

$$\mathcal{O}_{c',h,w}^{ViP} = \frac{\sum_{m,n=-1}^1 \mathcal{O}_{c',h+m,w+n}^{Zero}}{\sum_{m,n=-1}^1 \mathbb{1}(\mathcal{O}_{c',h+m,w+n}^{Zero} \neq 0)} \quad (4)$$

This is actually a convolution with $3 * 3$ filters, but with variable weight values depending on the number of non-expanding-zero neighbors. We can simplify the above computation by considering four cases similar to Equation 3:

$$\mathcal{O}_{c',h,w}^{ViP} = \begin{cases} \mathcal{O}_{c',h/2,w/2}^{Red} & h \text{ even, } w \text{ even} \\ \frac{1}{2}(\mathcal{O}_{c',\lfloor h/2 \rfloor, w/2}^{Red} + \mathcal{O}_{c',\lfloor h/2 \rfloor, w/2}^{Red}) & h \text{ odd, } w \text{ even} \\ \frac{1}{2}(\mathcal{O}_{c',h/2, \lfloor w/2 \rfloor}^{Red} + \mathcal{O}_{c',h/2, \lfloor w/2 \rfloor}^{Red}) & h \text{ even, } w \text{ odd} \\ \frac{1}{4}(\sum_{\substack{h=\lfloor h/2 \rfloor \text{ or } \lfloor h/2 \rfloor \\ w=\lfloor w/2 \rfloor \text{ or } \lfloor w/2 \rfloor}} \mathcal{O}_{c',h,w}^{Red}) & h \text{ odd, } w \text{ odd} \end{cases} \quad (5)$$

The above equations are embarrassingly parallel and hence fast to compute on GPU. We implemented our custom ViP layer based on Equation 5.

We can further provide an error bound, considering the case where we apply ViP to layer l_s .

Proposition 1. Assume the output of layer l_s (hence input to layer l_{s+1}), $\mathcal{O}^{(l_s)}$, is L -Lipschitz continuous (Li et al., 2017) on height and width dimensions (h, w) , i.e.,

$$|\mathcal{O}_{c,h_1,w_1}^{(l_s)} - \mathcal{O}_{c,h_2,w_2}^{(l_s)}| \leq L \| (h_1, w_1) - (h_2, w_2) \|_2, \text{ for } \forall h_1, h_2 \in [1, H], w_1, w_2 \in [1, W].$$

Assume that $\forall c', l$, the c' -th convolutional filter of the l -th layer, denoted as $\mathcal{W}_{c'}^{(l)}$, has a bounded l_2 -norm: $\|\mathcal{W}_{c'}^{(l)}\|_2 = \sqrt{\text{mean}^2(\mathcal{W}_{c'}^{(l)}) + \text{std}^2(\mathcal{W}_{c'}^{(l)})} \leq B^{(l)}$. Then, the l_2 -norm of the output error is bounded by:

$$\begin{aligned} & \|\mathcal{O}^{(l_e)ViP} - \mathcal{O}^{(l_e)Orig}\|_2 \\ & \leq \sqrt{2}L \sqrt{C^{(l_e)}H^{(l_e)}W^{(l_e)}} \prod_{l=l_s+1}^{l_e} \sqrt{C^{(l)}M^{(l)}B^{(l)}}, \quad (6) \end{aligned}$$

Algorithm 1 Virtual Pooling (ViP)

```

1: Input: model  $Net$ 
2: Output: ViP model  $ViPNET$ , Accuracy  $ViPA$ , Runtime  $ViPR$ 
3:
4: // Sensitivity analysis
5:  $i = 0$ 
6:  $ViPLayers = []$ 
7: for  $c$  in  $Net.ConvLayers$  do
8:    $A_c = evaluate(Net.ViP(c))$ 
9:    $ViPLayers.append((c, A_c))$ 
10: end for
11:  $ViPLayers.sorted(key = A_c, 'descending')$ 
12:
13: //Progressively interpolate and finetune
14:  $ViPA = [], ViPR = []$ 
15: for  $j = 0 : len(ViPLayers)$  do
16:    $Net = Finetune(Net.ViP(0 : j))$ 
17:    $ViPA.append(evaluate(Net))$ 
18:    $ViPR.append(time(Net))$ 
19: end for
20: Return  $ViPNET = Net, ViPA, ViPR$ 

```

where $C^{(l)}$ and $M^{(l)}$ are the number of input channels and kernel size of the l -th layer, respectively, and $C^{(l_e)}$ is the number of output channels of the l_e -th layer.

Proof. Deferred to Appendix. \square

If $\forall l > l_s, \sqrt{C^{(l)}}M^{(l)}B^{(l)} > 1$, the upper-bound will keep increasing when the output goes through multiple layers. This indicates that earlier ViP layers with more succeeding layers may have a bigger impact on the final output of the network and hence higher accuracy drop without finetuning. This actually reflects the intuition that perturbations from early layers will lead to higher error on the output as they propagate through the network. We will see this effect in both VGG-16 (Figure 2) and ResNet-50 (Figure 5).

3.2. ViP Algorithm

While speeding up CNNs can be achieved with ViP, it may also lead to some accuracy drop since interpolation is a method of approximation. Therefore, we propose the following procedure, as shown in Algorithm 1, as part of the ViP method to reduce the accuracy degradation while maximizing the speedup we can achieve via ViP. In Algorithm 1, we first do sensitivity analysis to detect which layers are less sensitive, in terms of the accuracy of the network, to the ViP operation (Line 7-10). For each of the conv layers c , we insert ViP immediately after it, and evaluate the network accuracy A_c without fine-tuning. The sensitivity is measured as the accuracy drop with respect to the original accuracy. A larger accuracy drop means that the layer is more sensitive to the ViP operation, while a lower accuracy drop means that the layer is robust to ViP. This is equivalent to sorting the sensitivity array A_i in descending order as shown in Line 11. We insert ViP layer after the ReLU immediately

following the conv layer, as both our experiments and prior work (Figurnov et al., 2016) show that inserting after ReLU gives better results. Our intuition is that by applying ViP before ReLU, we obtain less activations than the original without ViP and the network becomes less likely to identify smaller activation regions. Therefore, throughout the paper, whenever we mention inserting ViP after a certain conv layer, we mean inserting it after the ReLU layer that immediately follows it.

Based on the sorted per-layer sensitivity $ViPLayers$, we insert ViP layers progressively, and fine-tune the network after each interpolation to achieve a set of CNN models with different speedup-accuracy trade-offs (Line 15-19). For example, in the case of adding one ViP layer at a time, we add ViP after the $ViPLayers[0]$, fine-tune the model and obtain the first model, and then we add ViP after both $ViPLayers[0]$ and $ViPLayers[1]$, fine-tune the model and obtain the second model, and so on so forth. In this fashion, we will eventually generate $len(ViPLayers)$ models ($len(ViPLayers)$ is the total number of conv layers that we apply ViP to), all with different accuracy and runtime. However, repetitively fine-tuning the model $len(ViPLayers)$ times can be quite time-consuming, especially for large CNN models. To alleviate this problem, we conduct grouped fine-tuning, in which rather than progressively inserting ViP one layer at a time, we insert several ViP layers at a time (still based on sensitivity values). This results in fewer rounds, and hence less time, of fine-tuning, and both per-layer and grouped fine-tuning methods can generate different accuracy-speedup trade-offs for the baseline CNN model. An example of applying ViP to applications, such as a face detector in a mobile camera system is given in the supplementary material.

As it will be shown in Section 4, through the ViP method, we can speed up CNNs with minor accuracy drop. Furthermore, we can obtain a set of models with different speedup-accuracy trade-offs by applying ViP to various number of layers. As a result, our ViP method provides a knob for CNN practitioners to make trade-offs between accuracy and speedup based on the need of their applications. In addition, one can apply ViP on top of existing model acceleration methods, e.g., model compression (Han et al., 2015; Wen et al., 2016), CNN binarization (Ding et al., 2017; Rastegari et al., 2016), low rank approximation (Jaderberg et al., 2014; Lebedev et al., 2014), etc., to squeeze more performance out of the CNN models.

4. Experimental Results

In this section, we first describe the hardware and software setup of our experiments, and then present results to show the effectiveness of ViP method under:

Table 1. System Configurations for desktop and mobile platforms.

DESKTOP	
CPU/MAIN MEMORY	INTEL CORE-I7 / 32GB
GPU/MEMORY	NVIDIA TITAN X / 12GB
DL PLATFORM	CAFFE ON UBUNTU 14
MOBILE (NVIDIA JETSON TX1)	
CPU/MAIN MEMORY	QUAD ARM A57 / 4GB
GPU	NVIDIA MAXWELL ARCH
DL PLATFORM	CAFFE ON UBUNTU 14

1. Four CNN models: VGG-16 (Simonyan & Zisserman, 2014), ResNet-50 (He et al., 2016), All-CNN (Springenberg et al., 2014), Faster-RCNN with VGG-16 backbone (Ren et al., 2015).
2. Three datasets: ImageNet (Deng et al., 2009), CIFAR-10 (Krizhevsky et al., 2014), PASCAL-VOC (Everingham et al., 2010).
3. Two hardware platforms: Desktop and Mobile.
4. Two visual learning tasks: Image classification and object detection.

4.1. Experimental Setup

Throughout the experiments, we use Caffe (Jia et al., 2014) as our deep learning platform since its correctness has been validated by numerous research works. For fast training and inference, we implement a self-contained custom ViP layer in CUDA and integrate it into Caffe. The ViP layer inserts interpolated points between both columns and rows. The row and column size is doubled after interpolation and the resultant image size is enlarged four times. Interpolation is performed independently on points. This process is therefore embarrassingly parallel and can be easily accelerated by GPU. Each thread launched by the CUDA kernel processes one interpolated element. The thread block dimension order from fastest- to slowest-changing are column, row, channel, and batch to match the data layout in Caffe. Based on their position in the interpolated image, the points to be interpolated are classified into four types and estimated using Equation 5.

CNNs are now widely deployed and used in both cloud services and mobile phones, therefore we experiment with both a high-end desktop machine and a mobile platform with low power and energy profile. The detailed configurations are shown in Table 1. The desktop computer is equipped with high-end Intel Core-i7 CPU and Nvidia Titan X GPU, while the mobile platform is the Jetson TX1 comprised of efficient Quad-core ARM A57 CPU and Nvidia GPU with Maxwell architecture and 256 CUDA cores.

4.2. Image Classification

We first apply the ViP method to speedup and reduce the energy consumption of the image classification task.

4.2.1. ACCURACY AND SPEED

We experiment with state-of-the-art VGG-16 and ResNet-50 models using the ImageNet dataset. We first apply the ViP method on VGG-16 as described in Algorithm 1 in Section 3. We conduct sensitivity analysis to determine the per-layer sensitivity as shown in Figure 2. The x -axis labels provide the names of the layers being interpolated and we explicitly append “pool” in the name of the layers that are immediately preceding a pooling layer. As we can see, (1) after ViP insertion, different accuracy degradations without fine-tuning are obtained (shown on y -axis in Figure 2), (2) all layers immediately preceding a pooling layer exhibit the least sensitivity to ViP operation, which was also discovered by (Figurnov et al., 2016). The reason for this is that, although ViP loses information due to interpolation, many of those interpolated values are discarded by the pooling layer, and as a result, ViP has less impact on the final output of the network. And (3) besides the pooling layers, we can see a general trend of decreasing sensitivity when we insert ViP in later-stage layers. This follows the intuition that early perturbations lead to high error on the output when propagating through multiple layers, which is mathematically shown in Equation 6. The next step is to do model fine-tuning with progressively inserted ViP layers. We use grouped fine-tuning in the case of VGG-16 to save training time. Specifically, we have four rounds of fine-tuning according to the sensitivity of the layers: (1) in round one, we insert ViP after conv layers 13, 12, 10, 7, 2 and 4; (2) in round two, we further insert ViP after conv layers 11, 9 and 8; (3) in round three, we further insert ViP after conv layer 1; (4) in the final round four, we insert ViP layers after the remaining conv layers. Each round is initialized with the trained model from the previous round, because such an approach (1) gives slightly higher accuracy than fine-tuning from the baseline model and (2) saves training time.

Furthermore, we plot the training curve to illustrate how test accuracy recovers during grouped fine-tuning across four rounds, as shown in Figure 3. The zero line indicates the accuracy of the baseline network, and the y -axis is the accuracy improvement (degradation if negative) during fine-tuning. For fair comparison, we use top-5 accuracy for ImageNet throughout the paper as also reported in (Figurnov et al., 2016). The x -axis is the number of training iterations. We can see that after the initial insertion of ViP layers, there is a huge drop in accuracy. However, this gradually recovers during the fine-tuning step and even surpasses the original accuracy in round one. We conjecture that this is similar to the effect observed in (Han et al., 2016b), where linear interpolation serves as a type of regularization that improves network generalization.

After four rounds of grouped fine-tuning, we obtain four models of different speedup-accuracy trade-offs. A positive

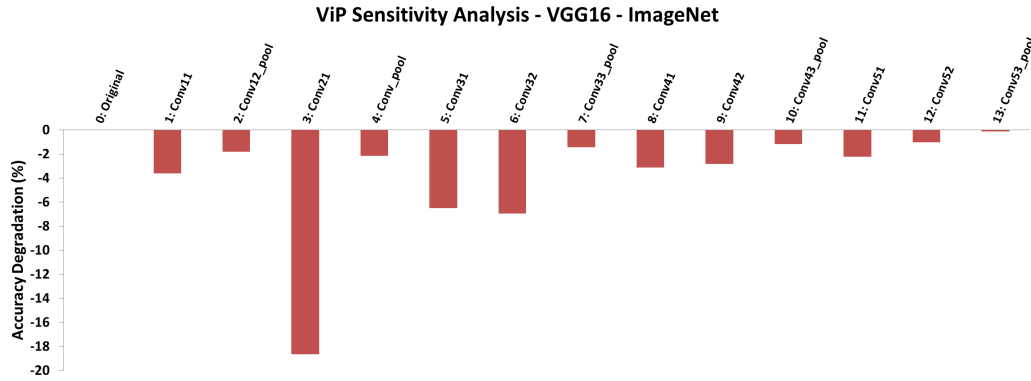


Figure 2. ViP sensitivity analysis of VGG-16 model under ImageNet dataset. For each of the conv layers, we insert ViP immediately after it, and evaluate the network accuracy without fine-tuning. The sensitivity is measured as the accuracy degradation.

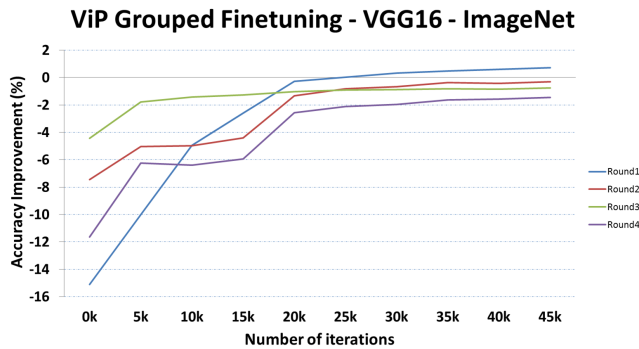


Figure 3. Four rounds of grouped finetuning of VGG-16 network using ImageNet dataset.

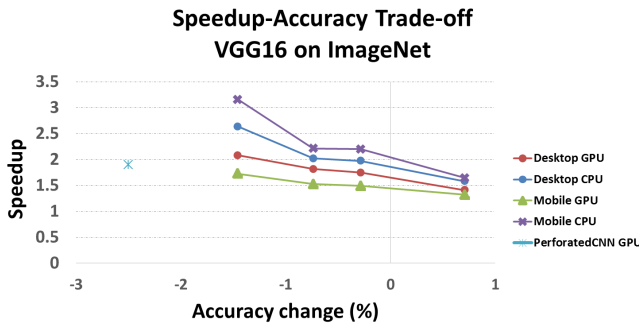


Figure 4. Speedup-Accuracy trade-off obtained by applying ViP on VGG-16 model with ImageNet dataset.

value for accuracy change means improvement, while a negative value means accuracy drop. Speedup is measured as the ratio of the inference time of the original model over the inference time of the model with ViP. We fine-tune the model with ViP on the desktop machine, because (1) storage of the mobile platform is insufficient for holding the entire ImageNet dataset, (2) training on desktop machine is significantly faster and the trained model can be evaluated on both desktop and mobile platforms for runtime analysis, and (3) model accuracy is platform-independent, which means once a model is obtained, its test accuracy remains the same on any platform. Accordingly, we can report accuracy and

speedup on both desktop and mobile platforms, while we only train the model on the desktop machine once.

We plot the results in Figure 4 along with the result of the previous state-of-the-art PerforatedCNNs (Furnov et al., 2016). Our method can achieve **2.1x** speedup with less than 1.5% accuracy degradation, while PerforatedCNNs can theoretically achieve 1.9x speedup with 2.5% accuracy degradation. The measured speedup of PerforatedCNNs is 2x when considering the reduced memory cost through implicit interpolation under Matlab implementation (Furnov et al., 2016). In the same way, ViP can also reduce memory transfer cost between layers thanks to the smaller-sized intermediate outputs by using larger-stride convolution. Unfortunately, Caffe does not support implicit interpolation and hence no memory saving of intermediate outputs as pointed out by PerforatedCNNs (GithubPerf). Therefore, for fair comparison, we eliminate the effect of memory saving in both implementations and use the theoretical upper-limit for PerforatedCNNs speedup since they did not report speedup on Caffe implementation. We expect ViP method to achieve even higher speedup in implementations that support implicit interpolation which saves memory transfer cost. In the case of mobile CPU, ViP is able to speed up the CNN by **3.16x** with less than 1.5% accuracy drop. Besides, what ViP can obtain is a set of models with different speedup-accuracy trade-offs rather than a single configuration, CNN practitioners can pick any of the models in Figure 4 that meets their need. Similarly, we apply ViP on ResNet-50 under ImageNet dataset. Figure 5 shows the results on sensitivity analysis and again we see the trend of decreasing sensitivity in later-stage layers. We have in total 53 conv layers because there are 49 conv layers on the primary branch and four on the bypass branches. Initially, we apply three rounds of grouped fine-tuning on ResNet-50. However, the final round, consisting of layers with the highest sensitivity, results in a steep accuracy drop, from -0.7% to -3.94% , we decide to use per-layer fine-tuning for the 12 layers in the last round to demonstrate the fine-grained progressive change in both accuracy and speed. Figure 6 shows the

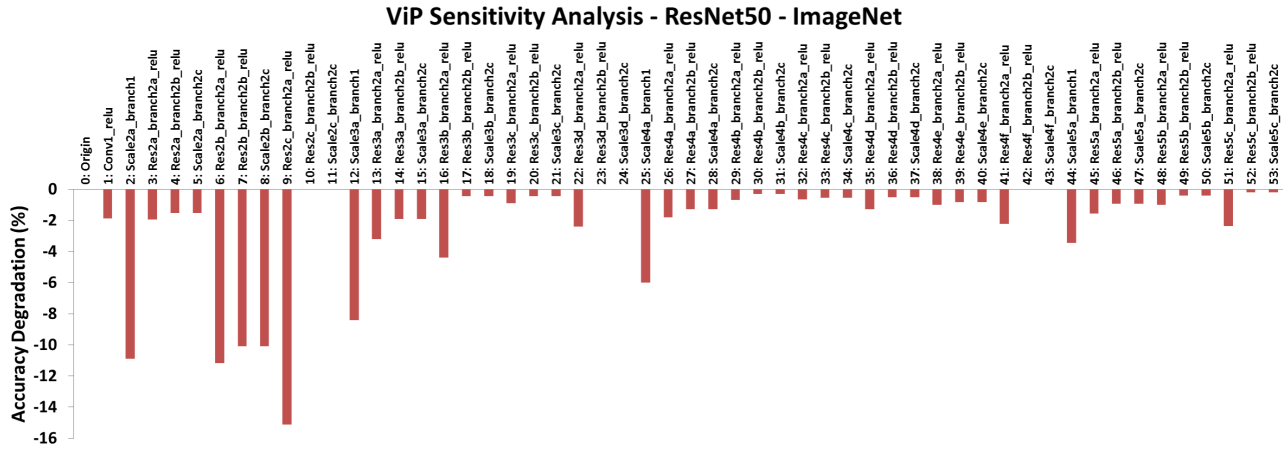


Figure 5. ViP sensitivity analysis of ResNet-50 model under ImageNet dataset. For each of the conv layers, we insert ViP immediately after it, and evaluate the network accuracy without fine-tuning. The sensitivity is measured as the accuracy degradation.

results. As expected, there is a clear trend of increasing speedup with higher accuracy drop when we insert more ViP layers. The speedup of mobile GPU and desktop GPU almost overlaps, and they both achieve **1.53x** speedup with less than 4% accuracy degradation. Meanwhile, mobile CPU obtains **2.3x** speedup at the same level of accuracy.

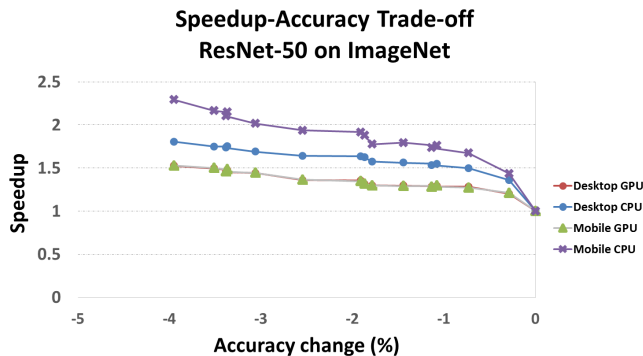


Figure 6. Speedup-Accuracy trade-off obtained by applying ViP on ResNet-50 model with ImageNet dataset.

Our results on the All-CNN network (Network All-CNN-C from (Springenberg et al., 2014)) show a **1.77x** speedup on the Titan X GPU and up to **3.03x** speedup on the mobile CPU, with desktop CPU and mobile GPU in between, while the top-1 accuracy drop is within 4%. Also, with less than 1% accuracy degradation, we obtain a **1.36x** speedup on Titan X GPU and 1.54x speedup on mobile CPU. Details are provided in the supplementary material.

4.2.2. POWER AND ENERGY

Mobile smart phones have dramatically changed human lives in the recent decade, and with the advent of convolutional neural networks, more and more mobile apps start to integrate visual tasks like image classification and object detection that heavily rely on CNNs. Other than speed, power and energy are the most critical constraints on mobile

platforms. Therefore, we further conduct experiments to see how ViP improves the power and energy profile on the mobile platform running CNN.

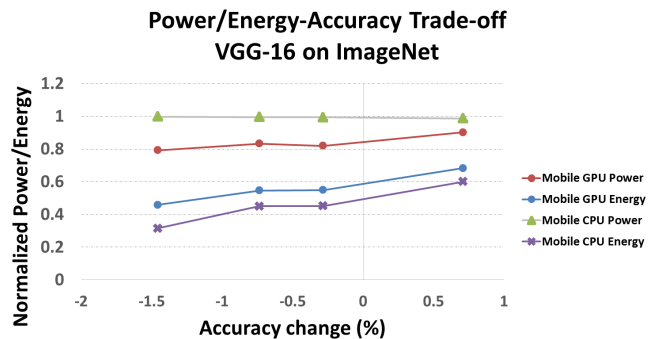


Figure 7. Power/Energy-Accuracy trade-off obtained by applying ViP on VGG-16 model with ImageNet dataset.

We first port both Caffe and our custom ViP layer to Jetson TX1. We use the on-board sensor to measure the power consumption of CNNs with and without ViP technique, and obtain the energy consumption by multiplying power by CNN latency. We test on all CNNs used previously, *i.e.*, All-CNN, VGG-16 and ResNet-50 (Detailed results on All-CNN are included in the supplementary material), and report their power/energy-accuracy trade-off curves in Figures 7 and 9, respectively. In each of the figures, we show four curves for power and energy consumption of either running CNN on mobile CPU or mobile GPU. We can see that, in terms of power, ResNet-50 has slightly lower power consumption on mobile GPU when using ViP and VGG-16 shows the highest power reduction of **21%** in mobile GPU power with ViP layers. In terms of energy consumption, VGG-16, All-CNN and ResNet-50 achieve up to **55%**, **46%** and **38%** mobile GPU energy reduction, respectively. Furthermore, All-CNN and VGG-16 can achieve up to **70%** CPU energy reduction while ResNet-50 tops at around **60%**.

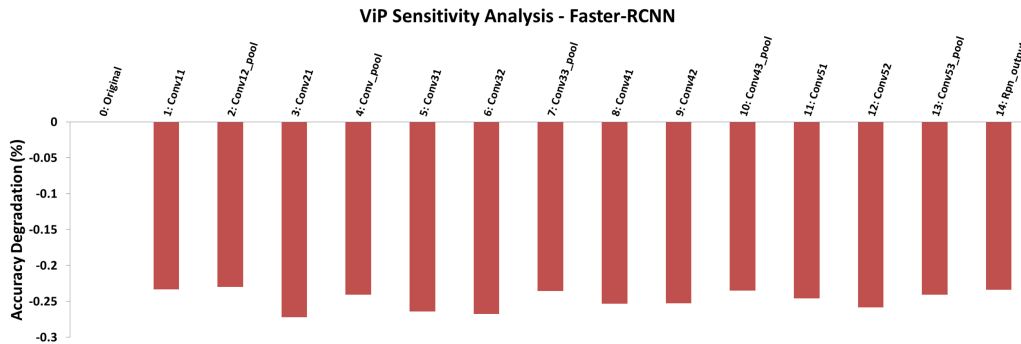


Figure 8. ViP sensitivity analysis of faster-rcnn with VGG-16 backbone under PASCAL VOC 2007 dataset. For each of the conv layers, we insert ViP immediately after it, and evaluate the accuracy without fine-tuning. The sensitivity is measured as the accuracy degradation.

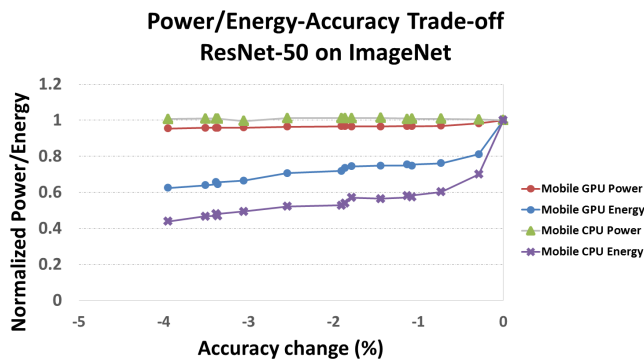


Figure 9. Power/Energy-Accuracy trade-off obtained by applying ViP on ResNet-50 model with ImageNet dataset.

4.3. Object Detection

In real-world applications, people may more often seek the functionality of object detection than image classification. However, much of the prior work on CNN model acceleration and compression only shows results on image classification (Wen et al., 2016; Ding et al., 2017; Lebedev et al., 2014). Although classification and detection share some common features like the early-stage convolutional layers, object detection has its unique components and challenges, *e.g.*, region proposal, bounding box regression, *etc.* Thus, without experimental results, it is hardly convincing to infer that methods excel on image classification can also work well on object detection tasks. Accordingly, in this section, we further test the ViP method on object detection task to show that it works across both important tasks.

We use the Caffe implementation of the state-of-the-art object detection framework faster-rcnn (Ren et al., 2015) with PASCAL VOC 2007 dataset, and integrate it with our custom ViP layer. We use VGG-16 as the backbone network of faster-rcnn as in (Ren et al., 2015). Similar to image classification task, we first analyze the sensitivity of each layers to ViP and the results are shown in Figure 8. Notice that, other than the conv layers from VGG-16, we also have one layer from the region proposal network, and this layer turns out to be among the least sensitive layers that we need to insert ViP in early fine-tuning rounds. The

mAP degradation from per-layer ViP ranges from $-0.23 \sim -0.27$, however, the recovered mAP degradation after fine-tuning is only down to -0.024 . Besides, we again observe that layers immediately followed by pooling are the most robust to ViP operation, as already discussed in the section of image classification. In the order of per-layer sensitivity, we conduct four rounds of grouped fine-tuning. As expected, with more layers followed by ViP operation, we are able to achieve higher speedup but with higher mAP degradation. In the end, we apply ViP to all conv layers and achieve **1.8x** speedup with 0.025 mAP degradation.

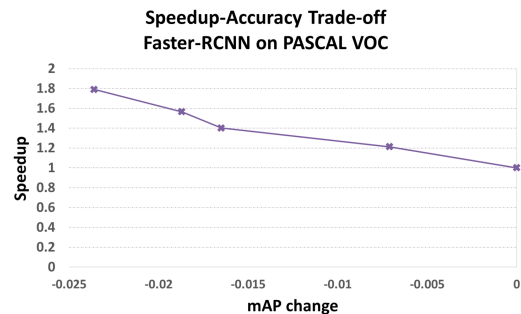


Figure 10. Speedup-Accuracy trade-off obtained by applying ViP on faster-rcnn with VGG-16 backbone under PASCAL VOC 2007.

5. Conclusion

In this work, we propose the Virtual Pooling(ViP) method that exploits the spatial redundancy of the input and reduces CNN computation by using a larger stride convolution and then recovering the output with linear interpolation (which is very efficient). We test and validate our method extensively on four CNN models, three representative datasets, both desktop and mobile platforms, and two primary learning tasks, *i.e.*, image classification and object detection. When running on Nvidia Titan X GPU, ViP is able to speedup VGG-16 by **2.1x** with less than 1.5% accuracy degradation in the image classification task, and speedup faster-rcnn by **1.8x** with 0.025 mAP degradation. Furthermore, we show that ViP is able to generate a set of models with different speedup-accuracy trade-offs. This provides CNN practitioners a tool for finding the model best suiting their needs.

References

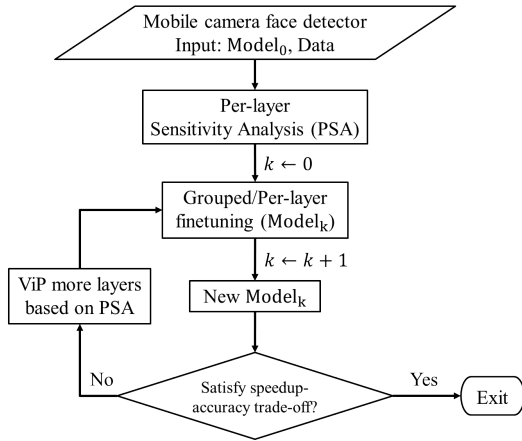
- Cai, E., Juan, D.-C., Stamoulis, D., and Marculescu, D. Neuralpower: Predict and deploy energy-efficient convolutional neural networks. In *Asian Conference on Machine Learning*, pp. 622–637, 2017.
- Courbariaux, M., Bengio, Y., and David, J.-P. Binaryconnect: Training deep neural networks with binary weights during propagations. In *Advances in neural information processing systems*, pp. 3123–3131, 2015.
- Courbariaux, M., Hubara, I., Soudry, D., El-Yaniv, R., and Bengio, Y. Binarized neural networks: Training deep neural networks with weights and activations constrained to +1 or -1. *arXiv preprint arXiv:1602.02830*, 2016.
- Deng, J., Dong, W., Socher, R., Li, L.-J., Li, K., and Fei-Fei, L. Imagenet: A large-scale hierarchical image database. In *Computer Vision and Pattern Recognition, 2009. CVPR 2009. IEEE Conference on*, pp. 248–255. IEEE, 2009.
- Denton, E. L., Zaremba, W., Bruna, J., LeCun, Y., and Fergus, R. Exploiting linear structure within convolutional networks for efficient evaluation. In *Advances in neural information processing systems*, pp. 1269–1277, 2014.
- Ding, R., Liu, Z., Shi, R., Marculescu, D., and Blanton, R. Lightnn: Filling the gap between conventional deep neural networks and binarized networks. In *Proceedings of the on Great Lakes Symposium on VLSI 2017*, pp. 35–40. ACM, 2017.
- Everingham, M., Van Gool, L., Williams, C. K., Winn, J., and Zisserman, A. The pascal visual object classes (voc) challenge. *International journal of computer vision*, 88(2):303–338, 2010.
- Figurnov, M., Ibraimova, A., Vetrov, D. P., and Kohli, P. Perforatedcnns: Acceleration through elimination of redundant convolutions. In *Advances in Neural Information Processing Systems*, pp. 947–955, 2016.
- GithubPerf. <https://github.com/mfigurnov/perforated-cnn-caffe>.
- Han, S., Pool, J., Tran, J., and Dally, W. Learning both weights and connections for efficient neural network. In *Advances in neural information processing systems*, pp. 1135–1143, 2015.
- Han, S., Liu, X., Mao, H., Pu, J., Pedram, A., Horowitz, M. A., and Dally, W. J. Eie: efficient inference engine on compressed deep neural network. In *Computer Architecture (ISCA), 2016 ACM/IEEE 43rd Annual International Symposium on*, pp. 243–254. IEEE, 2016a.
- Han, S., Pool, J., Narang, S., Mao, H., Gong, E., Tang, S., Elsen, E., Vajda, P., Paluri, M., Tran, J., et al. Dsd: Dense-sparse-dense training for deep neural networks. *arXiv preprint arXiv:1607.04381*, 2016b.
- He, K., Zhang, X., Ren, S., and Sun, J. Deep residual learning for image recognition. In *Proceedings of the IEEE conference on computer vision and pattern recognition*, pp. 770–778, 2016.
- He, Y., Kang, G., Dong, X., Fu, Y., and Yang, Y. Soft filter pruning for accelerating deep convolutional neural networks. *arXiv preprint arXiv:1808.06866*, 2018a.
- He, Y., Lin, J., Liu, Z., Wang, H., Li, L.-J., and Han, S. Amc: Automl for model compression and acceleration on mobile devices. In *Proceedings of the European Conference on Computer Vision (ECCV)*, pp. 784–800, 2018b.
- Jaderberg, M., Vedaldi, A., and Zisserman, A. Speeding up convolutional neural networks with low rank expansions. In *Proceedings of the British Machine Vision Conference. BMVA Press*, 2014.
- Jia, Y., Shelhamer, E., Donahue, J., Karayev, S., Long, J., Girshick, R., Guadarrama, S., and Darrell, T. Caffe: Convolutional architecture for fast feature embedding. In *Proceedings of the 22nd ACM international conference on Multimedia*, pp. 675–678. ACM, 2014.
- Krizhevsky, A., Nair, V., and Hinton, G. The cifar-10 dataset. *online: <http://www.cs.toronto.edu/kriz/cifar.html>*, 2014.
- Lebedev, V., Ganin, Y., Rakhuba, M., Oseledets, I., and Lempitsky, V. Speeding-up convolutional neural networks using fine-tuned cp-decomposition. *arXiv preprint arXiv:1412.6553*, 2014.
- Li, H., De, S., Xu, Z., Studer, C., Samet, H., and Goldstein, T. Training quantized nets: A deeper understanding. In *Advances in Neural Information Processing Systems*, pp. 5811–5821, 2017.
- LinkViz. <https://hackernoon.com/visualizing-parts-of-convolutional-neural-networks-using-keras-and-cats-5cc01b214e59>.
- Long, J., Shelhamer, E., and Darrell, T. Fully convolutional networks for semantic segmentation. In *Proceedings of the IEEE conference on computer vision and pattern recognition*, pp. 3431–3440, 2015.
- Rastegari, M., Ordonez, V., Redmon, J., and Farhadi, A. Xnor-net: Imagenet classification using binary convolutional neural networks. In *European Conference on Computer Vision*, pp. 525–542. Springer, 2016.

- Ren, S., He, K., Girshick, R., and Sun, J. Faster r-cnn: Towards real-time object detection with region proposal networks. In *Advances in neural information processing systems*, pp. 91–99, 2015.
- Sidiroglou-Douskos, S., Misailovic, S., Hoffmann, H., and Rinard, M. Managing performance vs. accuracy trade-offs with loop perforation. In *Proceedings of the 19th ACM SIGSOFT symposium and the 13th European conference on Foundations of software engineering*, pp. 124–134. ACM, 2011.
- Simonyan, K. and Zisserman, A. Very deep convolutional networks for large-scale image recognition. *arXiv preprint arXiv:1409.1556*, 2014.
- Springenberg, J. T., Dosovitskiy, A., Brox, T., and Riedmiller, M. Striving for simplicity: The all convolutional net. *arXiv preprint arXiv:1412.6806*, 2014.
- Wen, W., Wu, C., Wang, Y., Chen, Y., and Li, H. Learning structured sparsity in deep neural networks. In *Advances in Neural Information Processing Systems*, pp. 2074–2082, 2016.
- Wu, J., Leng, C., Wang, Y., Hu, Q., and Cheng, J. Quantized convolutional neural networks for mobile devices. In *Proceedings of the IEEE Conference on Computer Vision and Pattern Recognition*, pp. 4820–4828, 2016.
- Zhou, A., Yao, A., Guo, Y., Xu, L., and Chen, Y. Incremental network quantization: Towards lossless cnns with low-precision weights. *arXiv preprint arXiv:1702.03044*, 2017.
- Zhu, C., Han, S., Mao, H., and Dally, W. J. Trained ternary quantization. *arXiv preprint arXiv:1612.01064*, 2016.

000
001
002
003
004
005
006
007
008
009
010

Supplementary Material for “ViP: Virtual Pooling for Accelerating CNN-based Image Classification and Object Detection”

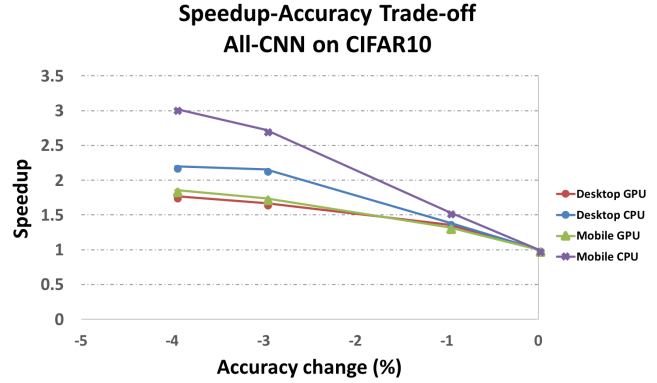
011 Figure 1 further illustrates how ViP method can be applied
012 to applications, such as a face detector in a mobile camera
013 system. In mobile phone cameras, a face detector can not
014 only show where the faces are, but also help camera auto-
015 focus for taking better pictures with people in sharp imaging.
016 Therefore, in this case lower accuracy can be tolerated as
017 long as some of the faces, if not all, are detected. At the same
018 time, there is also a speed requirement for camera to focus
019 as fast as possible. For such applications, we can generate
020 a set of models using the ViP method. We start from a
021 pre-defined or pre-trained model, *e.g.*, Faster-RCNN, and a
022 pre-collected dataset for human faces. Then we perform Per-
023 layer Sensitivity Analysis (PSA) to determine the sensitivity
024 of each conv layer in the network. Based on the sensitivity,
025 we can perform either grouped or per-layer fine-tuning to
026 generate new models with higher speedup until we obtain
027 the model that best satisfies the requirement on speedup-
028 accuracy trade-off.
029



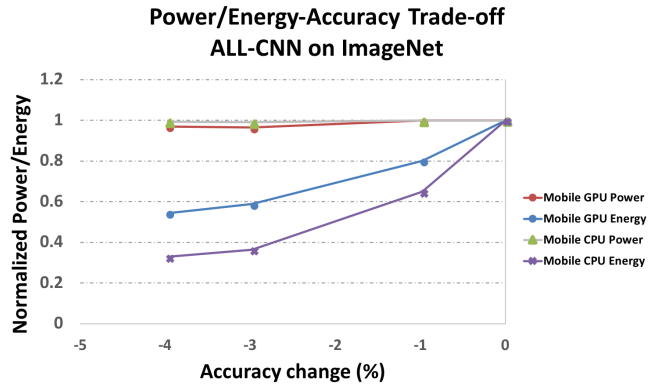
045 *Figure 1.* An example of applying ViP to the mobile phone camera
046 face detector. ViP progressively generates new models with
047 higher speedup until we obtain the model that best satisfies the
048 requirement on speedup-accuracy trade-off.
049

050
051 . AUTHORERR: Missing \icmlcorrespondingauthor.

052 Preliminary work. Under review by the International Conference
053 on Machine Learning (ICML). Do not distribute.
054



101 *Figure 2.* Speedup-Accuracy trade-off obtained by applying ViP
102 on All-CNN model with CIFAR-10 dataset.



201 *Figure 3.* Power/Energy-Accuracy trade-off obtained by applying
202 ViP on All-CNN model with CIFAR-10 dataset.

203 We also tried out our ViP method on the All-CNN network
204 (Network All-CNN-C from (Springenberg et al., 2014))
205 which consists of nine convolution layers without a fully-
206 connected layer and delivers high accuracy on CIFAR-10
207 dataset. With three rounds of ViP insertion and fine-tuning,
208 we obtain three models with different speedup-accuracy
209 trade-offs, as illustrated in Figure 2. We are able to achieve
210 **1.77x** speedup on the Titan X GPU and up to **3.03x** speedup
211 on the mobile CPU, with desktop CPU and mobile GPU
212 in between, while the top-1 accuracy drop is within 4%.
213 Also, with less than 1% accuracy degradation, we obtain
214 a **1.36x** speedup on Titan X GPU and **1.54x** speedup on
215

mobile CPU.

We port both Caffe and our custom ViP layer to Jetson TX1. We use the on-board sensor to measure the power consumption of CNNs with and without ViP technique, and obtain the energy consumption by multiplying power by CNN latency. We can see that, in terms of power, All-CNN has almost the same power on both CPU and GPU across all different ViP configurations. In terms of energy consumption, All-CNN achieves up to **46%** and **70%** energy reduction on mobile GPU and CPU, respectively.

To speedup the network, the upsampling overhead must be small so it does not offset the latency decrease resulting from the larger-stride convolution. ViP indeed works as an upsampling method and is thus similar to transposed convolution (Deconv) in terms of functionality. However, ViP is very fast with low runtime overhead (on average 4.7% of the network) and hence can achieve high speedup for the overall network. FCN (Long et al., 2015) uses Deconv to upsample, and its major drawback is its expensive computation. For example, consider a conv layer of input size $H * W * C$ ($H = W = 224$, $C = 3$) and $N = 64$ filters of size $M * M * C$ ($M = 3$). The MAC count for linear interpolation (after a stride 2 conv) is $(H/2 * W/2) * 2 * C * 2 + (H/2 * W/2) * C * 4 = 301,056$ (last three cases in Eq.5). The MAC count of Deconv (after a stride 2 conv) is $H * W * M * M * N * N = 1,849,688,064$ (We have two N s since the number of output channels after Deconv when used as upsampling should be the same as its input, which is $N = 64$ after stride 2 conv). We note that ViPs computation is only 0.016% of transposed convolution.

Proof for Proposition 1 is presented here.

Proof. We prove this bound by first bounding the error of the ViP layer $\mathcal{O}^{(l_s)}$, and then bounding the error accumulated to higher layers.

For the ViP layer $\mathcal{O}^{(l_s)}$, $\forall c, h, w$, the ViP error of $\mathcal{O}_{c,h,w}^{(l_s)}$ can be bounded:

$$\begin{aligned} & |\mathcal{O}_{c,h,w}^{(l_s)ViP} - \mathcal{O}_{c,h,w}^{(l_s)Orig}| \\ &= \frac{1}{K} \sum_{\substack{k=1 \\ (h_k, w_k) \in \mathcal{N}_{h,w}}}^K |\mathcal{O}_{c,h_k,w_k}^{(l_s)ViP} - \mathcal{O}_{c,h,w}^{(l_s)Orig}| \\ &\leq \frac{1}{K} \sum_{\substack{k=1 \\ (h_k, w_k) \in \mathcal{N}_{h,w}}}^K |\mathcal{O}_{c,h_k,w_k}^{(l_s)ViP} - \mathcal{O}_{c,h,w}^{(l_s)Orig}| \\ &\leq L * d_{max} = \sqrt{2}L \end{aligned} \quad (1)$$

where $\mathcal{N}_{h,w}$ is the set of neighbor locations of (h, w) that are averaged to compute the ViP value for pixel (h, w) , and d_{max} is the maximum l_2 -norm distance of the location

(c, h, w) and a neighbor location (c, h_k, w_k) , which is $\sqrt{2}$ in ViP.

Then, we bound the error accumulated from layer $l-1$ to l , i.e., $|\mathcal{O}_{c',h,w}^{(l)ViP} - \mathcal{O}_{c',h,w}^{(l)Orig}|$. Due to Eq. (1),

$$\begin{aligned} \mathcal{O}_{c',h,w}^{(l)ViP} &= \left(\sum_{c=1}^{C^{(l)}} \sum_{m,n=-\lfloor M^{(l)}/2 \rfloor}^{\lfloor M^{(l)}/2 \rfloor} \mathcal{O}_{c,s \cdot h - m, s \cdot w - n}^{(l-1)ViP} * \mathcal{W}_{c',c,m,n}^{(l)} \right)_+ \\ \mathcal{O}_{c',h,w}^{(l)Orig} &= \left(\sum_{c=1}^{C^{(l)}} \sum_{m,n=-\lfloor M^{(l)}/2 \rfloor}^{\lfloor M^{(l)}/2 \rfloor} \mathcal{O}_{c,s \cdot h - m, s \cdot w - n}^{(l-1)Orig} * \mathcal{W}_{c',c,m,n}^{(l)} \right)_+ \end{aligned} \quad (2)$$

where $(\cdot)_+$ is the ReLU activation function. Due to the fact that $\forall x, y \in R, |(x)_+ - (y)_+| \leq |x - y|$, we have:

$$\begin{aligned} & |\mathcal{O}_{c',h,w}^{(l)ViP} - \mathcal{O}_{c',h,w}^{(l)Orig}| \\ &\leq \left| \sum_{c=1}^{C^{(l)}} \sum_{m,n=-\lfloor M^{(l)}/2 \rfloor}^{\lfloor M^{(l)}/2 \rfloor} (\mathcal{O}_{c,s \cdot h - m, s \cdot w - n}^{(l-1)ViP} - \mathcal{O}_{c,s \cdot h - m, s \cdot w - n}^{(l-1)Orig}) \mathcal{W}_{c',c,m,n}^{(l)} \right| \end{aligned} \quad (3)$$

Using Cauchy-Schwarz inequality, we have:

$$\begin{aligned} & |\mathcal{O}_{c',h,w}^{(l)ViP} - \mathcal{O}_{c',h,w}^{(l)Orig}| \\ &\leq \sqrt{\sum_{c=1}^{C^{(l)}} \sum_{m,n=-\lfloor M^{(l)}/2 \rfloor}^{\lfloor M^{(l)}/2 \rfloor} (\mathcal{O}_{c,s \cdot h - m, s \cdot w - n}^{(l-1)ViP} - \mathcal{O}_{c,s \cdot h - m, s \cdot w - n}^{(l-1)Orig})^2} \\ &\quad * \sqrt{\sum_{c=1}^{C^{(l)}} \sum_{m,n=-\lfloor M^{(l)}/2 \rfloor}^{\lfloor M^{(l)}/2 \rfloor} \mathcal{W}_{c',c,m,n}^{(l)}} \\ &\leq \sqrt{C^{(l)} M^{(l)} B^{(l)}} \max_{c',h,w} |\mathcal{O}_{c,h,w}^{(l-1)ViP} - \mathcal{O}_{c,h,w}^{(l-1)Orig}| \end{aligned} \quad (4)$$

Therefore, accumulating the error from the ViP layer l_s to layer l_e , we have:

$$|\mathcal{O}_{c',h,w}^{(l_e)ViP} - \mathcal{O}_{c',h,w}^{(l_e)Orig}| \leq \sqrt{2}L \prod_{l=l_s+1}^{l_e} \sqrt{C^{(l)} M^{(l)} B^{(l)}}, \quad (5)$$

Thus, the l_2 -norm of the output error is bounded by:

$$\begin{aligned} & \|\mathcal{O}^{(l_e)ViP} - \mathcal{O}^{(l_e)Orig}\|_2 \\ &\leq \sqrt{2}L \sqrt{C^{(l_e)} H^{(l_e)} W^{(l_e)}} \prod_{l=l_s+1}^{l_e} \sqrt{C^{(l)} M^{(l)} B^{(l)}}. \end{aligned} \quad (6)$$

□

References

- 110
111 Long, J., Shelhamer, E., and Darrell, T. Fully convolutional
112 networks for semantic segmentation. In *Proceedings*
113 *of the IEEE conference on computer vision and pattern*
114 *recognition*, pp. 3431–3440, 2015.
115
- 116 Springenberg, J. T., Dosovitskiy, A., Brox, T., and Ried-
117 miller, M. Striving for simplicity: The all convolutional
118 net. *arXiv preprint arXiv:1412.6806*, 2014.
119
120
121
122
123
124
125
126
127
128
129
130
131
132
133
134
135
136
137
138
139
140
141
142
143
144
145
146
147
148
149
150
151
152
153
154
155
156
157
158
159
160
161
162
163
164